Soft Matter

Accepted Manuscript

ROYAL SOCIETY OF CHEMISTRY

www.rsc.org/softmatter

Structure and Flow of Dense Suspensions of Protein Fractal Aggregates in Comparison with Microgels.

Walailuk Inthavong, Anna Kharlamova, Christophe Chassenieux, Taco Nicolai

LUNAM Université du Maine, IMMM UMR-CNRS 6283, Polymères, Colloïdes et Interfaces, *72085 Le Mans cedex 9, France*

Abstract

Solutions of the globular whey protein β-lactoglobulin (β-lg) were heated at different protein concentrations leading to the formation of polydisperse fractal aggregates with different average sizes. The structure of the solutions was analyzed with light scattering as a function of the protein concentration. The osmotic compressibility and the dynamic correlation length decreased with increasing concentration and became independent of the aggregate size in dense suspensions. Results obtained for different aggregate sizes could be superimposed after normalizing the concentration with the overlap concentration. Dense suspensions of fractal protein aggregates are strongly interpenetrated and can be visualized as an ensemble of fractal 'blobs'. The viscosity of heated β-lg solutions increased extremely sharply above 80 g/L and diverged at 98 g/L, mainly due to the sharply increasing aggregate size. At fixed aggregate size, the viscosity increased initially exponentially with increasing concentration and then diverged. The increase was stronger when the aggregates were larger, but the dependence of the viscosity on the aggregate size was weaker than that of the osmotic compressibility and the dynamic correlation length. The concentration dependence of the viscosity of solutions of fractal β-lg aggregates is much stronger than that of homogeneous β-lg microgels. The behavior of fractal aggregates formed by whey protein isolate was similar.

Introduction

Globular proteins may be considered as dense nanoparticles that are stabilized in aqueous solutions by electrostatic repulsion. Heating aqueous protein solutions renders the rigid structure of the globular proteins mobile which may allows formation of bonds between

the proteins and can cause irreversible aggregation. Aggregation leads to the formation of a percolating network above a critical gel concentration (C_g), but at lower concentrations stable suspensions of finite size aggregates are obtained[1-2]. The size of the aggregates increases with increasing protein concentration and diverges at C_g. The local structure of the aggregates and the value of C_g depend on the type of protein, the pH and the added salt. However, for a number of different globular proteins it has been shown that the large scale structure of the aggregates is self-similar[3-9]. Self-similar aggregates are characterized by their fractal dimension (d_f) which relates the molar mass (M) to the radius (R): $M \propto R^{df}$. The value of d_f was found to increase weakly from 1.7 when electrostatic interaction are strong to 2.0 when they are weak, but it does not depend on the type of protein.

Fractal protein aggregates have been studied extensively in dilute solutions, but as far as we are aware no systematic investigation has been done on the flow properties of dense suspensions of such aggregates. More in general, while dense suspensions of homogeneous spherical particles have been investigated in much detail [10-13], dense suspensions of fractal aggregates have received relatively little attention [14-17]. An important difference between homogeneous particles and fractal aggregates is that the density of the former does not depend on their size, but for the latter it decreases with increasing size. Considering that the aggregates are spherical we may define their density as $\rho=3M/(4\pi N_a R^3)$, with N_a Avogadro's number so that $\rho \propto R^{df-3}$. It has therefore been suggested that the viscosity of dense fractal aggregates can be understood in the same way as for homogeneous particles, by treating them as particles with a lower density. However, since fractal aggregates have an open structure, they are to certain extent interpenetrable. This is especially important for fractal globular protein aggregates, which are very polydisperse, and are strongly interpenetrated in dense suspensions. In addition, it has been shown that fractal protein aggregates have some degree of flexibility [18]. Recently, it was demonstrated that interpenetration and flexibility of the fractal aggregates has important effects on the viscosity in dense suspensions[19].

Here we present an investigation of the structure and the viscosity as a function of concentration for aqueous suspensions of fractal globular protein aggregates with different sizes. We will compare the viscosity of fractal aggregates with that of microgels formed by the same proteins [20], which enables a direct assessment of the effect of the structure of protein particles. The globular protein used in this investigation was β-lactoglobulin (β-lg), which is the main component of whey. Stable suspensions of aggregates with different average sizes were formed by heating aqueous β-lg solutions at different protein concentrations at pH 7.0

until steady state was reached. It has already been reported elsewhere that at these conditions β-lg forms initially small curved strands with a hydrodynamic radius $R_h \approx 15$nm. At higher protein concentrations these strands randomly associate into self similar aggregates with $d_f=1.7$. In order to render our findings more relevant for applications we have compared the results obtained for aggregates formed by pure β-lg with those formed by a commercial whey protein isolate.

Materials and methods

Materials

The β-lactoglobulin (Biopure, lot JE 001-8-415) used in this study was purchased from Davisco Foods International, Inc. (Le Sueur, MN, USA) and consisted of approximately equal quantities of variants A and B. Whey protein isolate (WPI) powder was purchased from Lactalis (Laval, France), which contained 95% protein on dry weight basis of which 70% β-lg and 20% α-lactalbumin. The molar masses of β-lactoglobulin and α-lactalbumin are 18 kg/mol and 14 kg/mol, respectively [21]. The powders were dissolved in Milli-Q water to which 200 ppm NaN_3 was added to prevent bacterial growth. The pH of the solution was adjusted to 7 by adding small amounts of NaOH 0.1 M. For light scattering; dilute solutions were filtered through 0.2 μm pore size Anotop filters. The protein concentration was determined by UV absorption at 278 nm using extinction coefficient 0.96 $Lg^{-1}cm^{-1}$ and 1.05 $Lg^{-1}cm^{-1}$ for β-lg and WPI, respectively. Protein solutions were concentrated by ultrafiltration utilizing the KrosFlo Research II/i/Tangential Flow Filtration (TFF) System (Spectrum Europa B.V.)

Light scattering

Light scattering measurements were done using an ALV-5000 multibit, multitau, full digital correlator in combination with a laser emitting vertically polarized light at $\lambda = 632$ nm (ALV-Langen). The temperature was controlled by a thermo-stat bath to within ± 0.1 °C. The relative excess scattering intensity (I_r) was determined as the total intensity minus the solvent scattering divided by the scattering of toluene at 20°C. I_r is related to the osmotic compressibility ($(d\pi/dC)^{-1}$) and the z-average structure factor (S(q)) [22-23]:

$$I_r = K.C.RT.(d\pi/dC)^{-1}S(q) \quad (1)$$

with R the gas constant and T the absolute temperature and q the scattering wave vector.

$$K = \frac{4\pi^2 n^2}{\lambda^4 N_a}.\left(\frac{dn}{dC}\right)^2.\left(\frac{n_s}{n}\right)^2.\frac{1}{R_s} \quad (2)$$

where (dn/dC) is the refractive index increment, and R_s is the Rayleigh ratio of toluene. $(n_s/n)^2$ corrects for the difference in scattering volume of the solution with refractive index n and toluene with refractive index n_s. S(q) describes the dependence of I_r on the scattering wave vector: $q=(4\pi n/\lambda).\sin(\theta/2)$, with θ the angle of observation. We used dn/dC= 0.189 cm^3/g and $R_s= 1.35\times10^{-5}cm^{-1}$. In dilute solutions and in the limit of $q\rightarrow0$, I_r/KC is equal to the weight average molar mass (M_w). At finite concentrations we measure an apparent molar mass (M_a) that is proportional to the osmotic compressibility: $M_a=RT/(d\pi/dC)$. The initial concentration dependence of M_a can be expressed in terms of a virial expansion:

$$M_a=M_w/(1+2A_2M_wC+\ldots) \quad (3)$$

The initial q-dependence of the structure factor extrapolated to $C\rightarrow0$ can be used to obtain the z-average radius of gyration (R_g):

$$S(q)=(1+q^2.R_g^2/3)^{-1} \quad (4)$$

At higher concentrations, when interactions cannot be neglected, the initial q-dependence of structure factor can be expressed in terms of the static correlation length (ξ_s):

$$S(q)=(1+q^2.\xi_s^2)^{-1} \quad (5)$$

The normalized intensity autocorrelation ($g_2(t)$) that is measured with dynamic light scattering (DLS) is related to the normalized electric field correlation function, $g_1(t)$: $g_2(t)=1+g_1(t)^2$ [24]. $g_1(t)$ was analyzed in terms of a distribution of relaxation times using the REPES routine [25]:

$$g_1(t) = \int A(log\tau)\exp(-t/\tau)d\log\tau \quad (5)$$

In all cases monomodal distributions were observed and the correlograms could be well described using the following an analytical expression for A(logτ):

$$A(\log\tau) = k\tau^p \exp\left[-\left(\tau/\tau^*\right)^s\right] \quad (6)$$

In binary solutions the relaxation of the intensity fluctuations is caused by cooperative diffusion of the solute and cooperative diffusion coefficient can be calculated from the average relaxation rate: $D_c = (q^2.\tau)^{-1}$. The dynamic correlation length (ξ_d) can be calculated from D_c at $q \rightarrow 0$:

$$D_c = \frac{kT}{6\pi\eta\xi_d} \quad (7)$$

with η the viscosity, k Boltzman's constant, and T the absolute temperature. When interactions can be neglected, i.e. at low concentrations, ξ_d is equal to the z-average hydrodynamic radius. We note that the z-average values of R_h and R_g determined by light scattering give strong weight to the larger particles in the distribution and even more so for R_g than for R_h.

Rheology

The viscosity was measured as a function of the shear rate using a rheometer (AR2000, TA Instruments) with a cone and plate or a couette geometry. After loading the samples were pre-sheared at 100 s^{-1} during 1 min. The viscosity was determined during subsequent shear ramps with increasing and decreasing shear rates. The results obtained with increase and decreasing shear rates were found to be the same. Measurements done using the cone and plate geometry showed an upturn at low shear rates, which was due to the formation of a weak elastic surface layer of proteins. In ref. [26] it was shown that this effect can be much reduced by using a couette geometry. Therefore for one series of samples we have used both geometries and found that indeed the artificial increase was no longer observed. Nevertheless, the same results can be obtained with both geometries after superposition of the data at

different concentrations, see Supplementary Information. As a much larger quantity of solution is needed for the couette geometry, we have used for the other series of measurements the cone and plate geometry.

Results

Characterization of the aggregates.

Fractal aggregates of β-lg with different sizes were prepared by heating at 80°C aqueous solutions with different protein concentrations at pH 7.0 until steady state was reached. At steady state all proteins are denatured and for C>40g/L more than 90% of the proteins form aggregates[18]. The remaining proteins are present in the form of monomers, dimers and trimers. As was mentioned in the Introduction, detailed investigations of the fractal structure of aggregates formed by heating β-lg or WPI in aqueous solution have already been reported elsewhere[3-4, 18]. Characterization of the aggregates used for the present investigation by light scattering showed that their structure was same as that reported in the literature.

The weight average molar mass (M_w) of the aggregates was determined using light scattering as described in the Material and Methods section. The dependence of M_w on the concentration at which the aggregates were formed is shown in figure 1a. At low concentrations relatively monodisperse strands were formed, but for C>40g/L, random aggregation of these strands led to an increase of M_w with increasing concentration. The molar mass diverged at a critical gel concentration C_g=98g/L. The z-average radius of gyration (R_g) and the z-average hydrodynamic radius (R_h) increased with increasing M_w following a power law, which is expected for fractal aggregates, see figure 1b. The dependence of both R_h and R_g on M_w is compatible with d_f=1.7, but R_h is systematically smaller than R_g by a factor of about 0.7, in agreement with findings reported earlier [18]. The principal reason for this difference is the polydispersity of the aggregates, R_g is derived from the z-average of R_g^2 and R_h from the z-average of R_h^{-1}. Therefore R_g is more sensitive to larger aggregates.

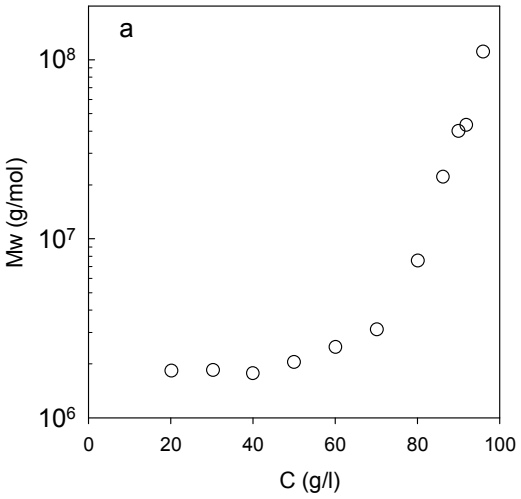

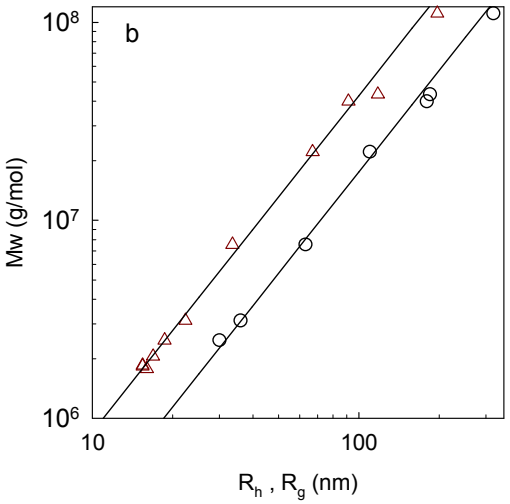

Fig. 1a Molar mass of β-lg aggregates formed in heated aqueous solutions as a function of the protein concentration.

Fig. 1b Dependence of the molar mass of β-lg aggregates on the radius of gyration (circles) or the hydrodynamic radius (triangles).

Structure of the aggregate solutions

All solutions of fractal aggregates were optically clear and their structure was studied with light scattering over a range of concentrations. Fig. 2 shows I_r/KC for large aggregates that were formed by heating at C=96 g/L and that were subsequently progressively diluted. At high protein concentrations the structure factor was independent of q in the range covered by light scattering, implying that the correlation length of the concentrated solutions was less

than 15nm. It was shown elsewhere[27] using small angle X-ray scattering experiments that the structure factor of concentrated aggregate solutions shows a peak implying a certain degree of order in the distribution of the proteins. The osmotic compressibility and the correlation length of the concentration fluctuations increased with decreasing concentration causing an increase of I_r/KC and a stronger q-dependence.

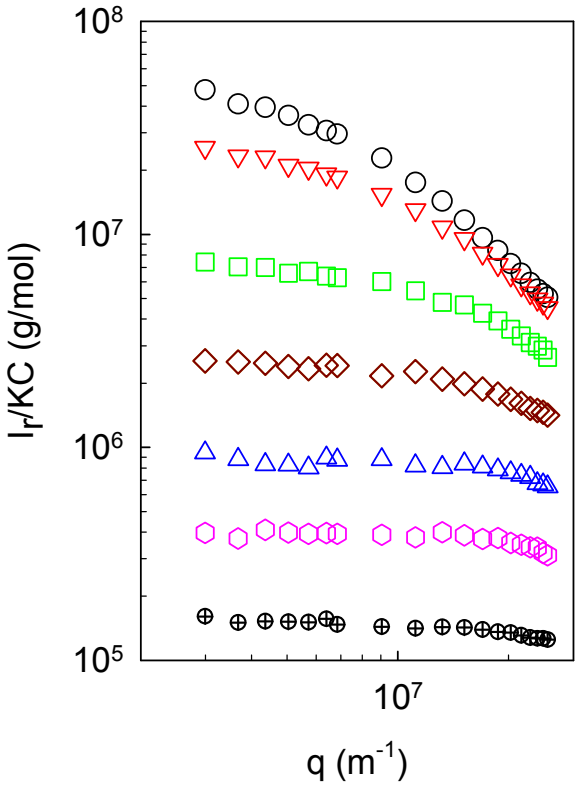

Fig. 2 Dependence of I_r/KC on q for aggregates formed by heating at C=96 g/L and subsequently diluted to different concentrations as indicated in the figure.

Fig. 3a shows the concentration dependence of the apparent molar mass ($M_a = I_r/KC_{(q\to 0)}$) for protein aggregates with different sizes obtained by heating at different concentrations. As was mentioned above, M_a is proportional to the osmotic compressibility and is equal to M_w if interactions are negligible, i.e. at low concentrations. In all cases the osmotic compressibility decreased with increasing concentration, due to electrostatic and excluded volume interactions between the aggregates and at the highest concentrations M_a became independent of the aggregate size. The latter implies that in dense suspensions the

aggregates are strongly interpenetrated and that the osmotic compressibility is determined by interaction between the elementary units of the aggregates.

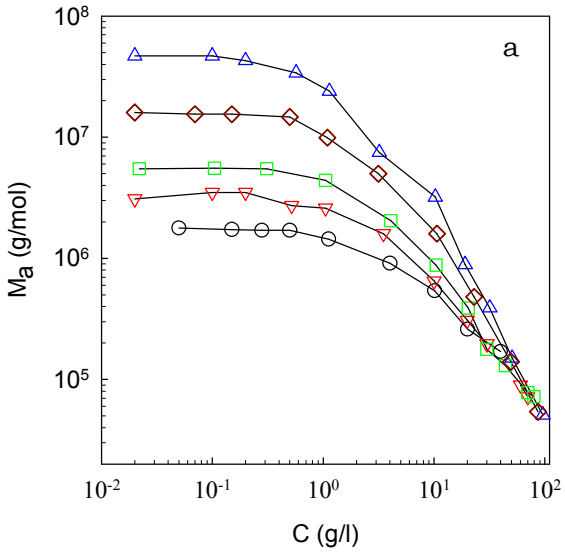

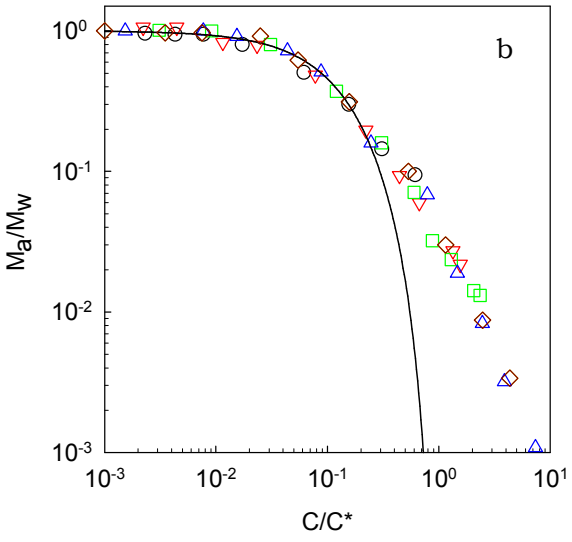

Fig.3a Concentration dependence of M_a for aggregates formed by heating at different protein concentrations indicated in the figure. The same data are plotted in fig. 3b after normalizing M_a with M_w and C with C. The solid line in fig. 3b represents eq.8.*

For non-interacting hard spheres, M_a/M_w can be well described by the following equation[28]:

$$\frac{M_a}{M_w} = \frac{(1-\phi)^4}{1+4\phi+4\phi^2-4\phi^3+\phi^4} \quad (8)$$

where ϕ is the volume fraction of the particles. For solutions of polydisperse soft particles such as the protein aggregates, the initial concentration dependence of M_a/M_w can still be described by eq.8 if for ϕ we use an effective volume fraction: $\phi_e=C/C^*$, where C^* is the concentration at which the effective volume fraction of the particles is unity and is related to the second virial coefficient: $C^*=A_2/(4M_w)$. When expressed in units of volume the second virial coefficient is 4 times the effective volume of the particles. Fig. 3b shows that eq.8 describes the results in this representation up to $C/C^*\approx0.2$. At higher protein concentrations, M_a decreased less steeply than for equivalent hard spheres, because the aggregates are polydisperse and can interpenetrate. As expected, the values of C^* decreased with increasing aggregate size, see fig. 4.

For spherical particles C^* can also be calculated from their molar mass and their radius:

$$C^*=3M_w/(4\pi R^3 N_a). \quad (9)$$

For monodisperse non-interacting hard spheres the two methods give the same value, but for polydisperse or interacting particles they will be different. For the polydisperse protein aggregates studied here, the values calculated using eq. 9 are smaller if one uses R_g for the radius than if one uses R_h, see fig. 4. The values of C^* obtained from the comparison of the concentration dependence of M_a with eq. 8 were intermediate between those calculated using eq. 9 with $R=R_h$ or $R=R_g$. However, the molar mass dependence was weaker, which is a consequence of the increasing polydispersity with increasing M_w.

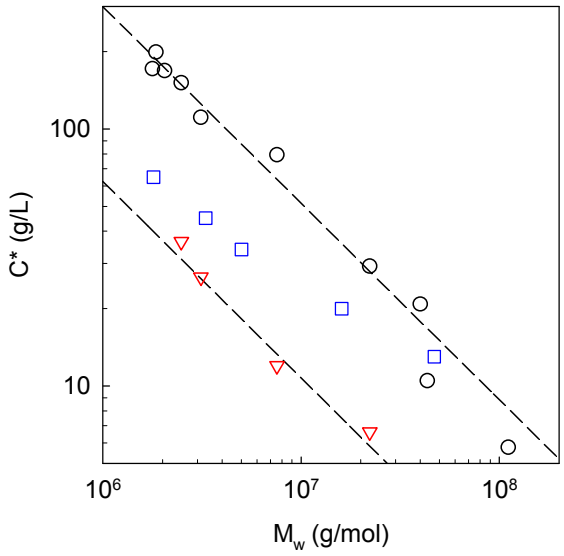

Fig. 4. Dependence of C on the molar mass for fractal β-lg aggregates. The data obtained from fits of the initial concentration dependence of M_a to eq. 8 are indicated by squares, whereas the circles and the triangles indicate the values calculated using eq. 9 with R_h and R_g, respectively. The dashed lines indicate the power law dependence corresponding to the one shown in fig. 1b.*

As can be seen in fig.2, interpenetration of the aggregates caused a decrease of the correlation length with increasing concentration. At higher concentrations, the static correlation length became too small to be determined with light scattering, but the dynamic correlation length (ξ_d) obtained from dynamic light scattering could be determined over the whole concentration range. Examples of correlograms and the corresponding relaxation time distributions are shown in fig. S3 of the supplementary information. As was discussed in ref. [18], in dilute solutions the q-dependence of the diffusion coefficient increases with increasing aggregate size, because the fractal aggregates are semi-flexible. With increasing concentration the q-dependence of D_c decreased, because the correlation length of the concentration fluctuations decreased, see fig.S4 of the supplementary information. ξ_d obtained from the cooperative diffusion coefficient extrapolated to zero-q, see eq.7, decreased with increasing concentration down to values approaching the radius of monomeric β-lg that is about 2nm. Fig. 5 shows that ξ_d has the same power law dependence on M_a as R_h on M_w independent of the aggregate size. The structure of the interpenetrated aggregate solution can thus be visualized as an ensemble of fractal 'blobs' with radius ξ_d and molar mass M_a, independent

of the aggregate size. The peak in the structure factor at larger q-values that was found with SAXS [27] implies that the 'blobs' are regularly distributed in salt free solutions.

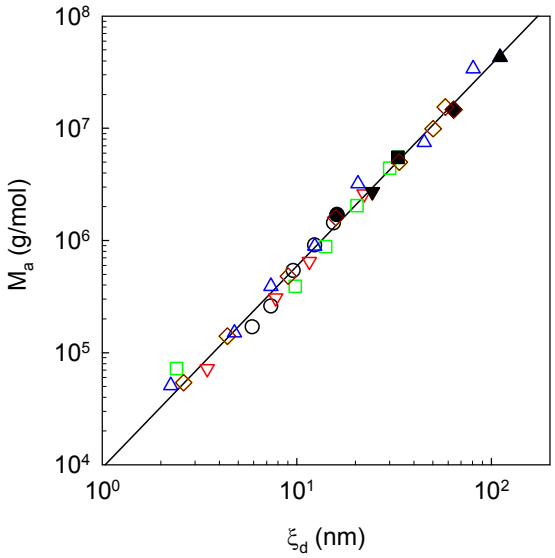

Fig. 5 Dependence of the apparent molar mass on the dynamic correlation length for solutions of aggregates with different sizes measured at different protein concentrations. The filled symbols represent values at infinite dilutions where M_a=M_w and ξ_d=R_h. The solid line has slope 1.7. The symbols are as in fig.3a.

Viscosity

Solutions of β-lg at different concentrations were loaded on the rheometer after heating and the viscosity (η) was determined as a function of the shear rate ($\dot{\gamma}$). For the more viscous solutions we observed shear thinning at larger shear rates, see fig.6a. We also observed an increase of the viscosity with decreasing shear rate at low shear rates. However, as was mentioned in the materials and methods section, this increase is an artifact caused by the formation of a layer of proteins at the interface. If we ignore the artificial increase at low shear rates, the results obtained at different concentrations can be superimposed by horizontal and vertical shift factors, see fig. 6b. This allowed us to obtain the limiting low shear viscosity (η_0) at all concentrations.

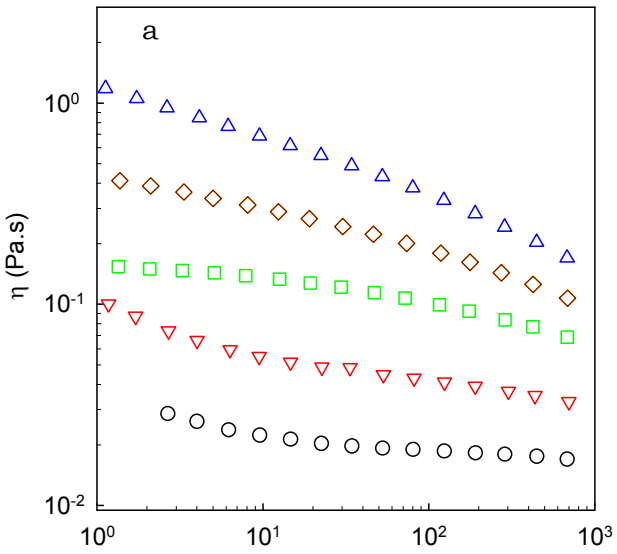

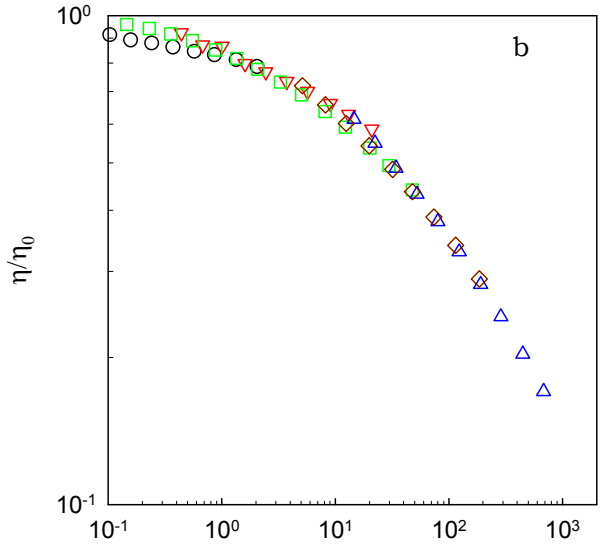

Fig. 6a Shear rate dependence of the viscosity of heated β-lg solutions at different concentrations. Fig. 6b shows a master curve of the same data obtained by horizontal and vertical shifts with respect to the data at C=96 g/L. The artificial upturns at low shear rates were removed from the master curve.

η_0 increased very sharply with increasing protein concentration for C>70g/L and diverged at the gel concentration, see fig. 7a. The sharp increase of η_0 was caused by a combination of increasing protein concentration and increasing aggregate size. In order to distinguish these two effects, we measured the shear rate dependent viscosity as a function of the protein concentration keeping the aggregate size fixed. To this end, a solution of aggregates formed at C=96g/L with R_g=320 nm was progressively diluted. Master curves could be obtained by superposition of the results obtained at different dilutions, see supplementary results. The concentration dependence of η_0 for the aggregates with fixed size formed at C=96g/L and subsequently diluted is compared in fig. 7a with that of aggregates with different sizes formed at different concentrations. Even though the concentration dependence of η_0 for solutions with the same large aggregates was steep, it was much more progressive than that of aggregates formed at different concentrations. This clearly demonstrates that the effect of increasing the aggregate size is more important than the effect of increasing the protein concentration. Similar results were obtained with a commercial WPI sample, see fig. 7b, which is not surprising, because WPI forms similar fractal aggregates in heated aqueous solutions[4]. The WPI solutions gelled at a slightly lower protein concentration (95g/L) and therefore the steep increase of the viscosity occurred at slightly lower concentrations. In the following we focus on the results obtained with pure β-lg.

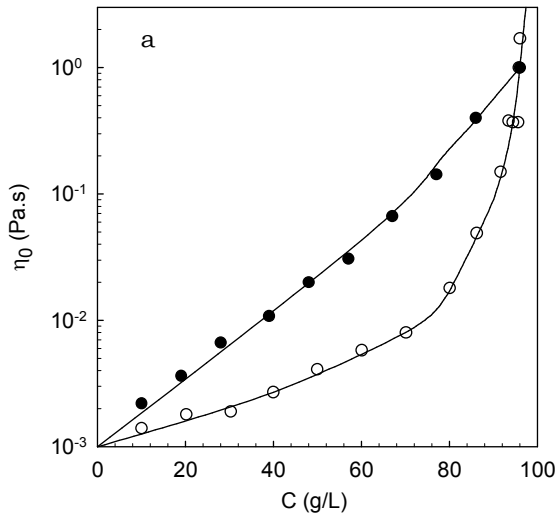

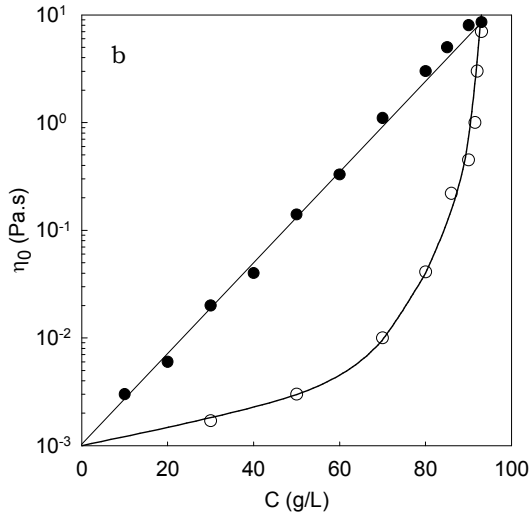

Fig.7a Zero shear rate of the viscosity for β-lg solutions that were heated at different concentrations (open symbols) or that were heated at C=96 g/L and subsequently diluted (closed symbols). Fig. 7b shows the results obtained for WPI heated at different concentrations (open symbols) or that were heated at C=93 g/L and subsequently diluted (closed symbols).

In order to investigate the effect of the average aggregate size on the concentration dependence of η_0, solutions with different β-lg concentrations were heated. The viscosity of each system was subsequently measured as a function of the protein concentration by dilution. The smaller aggregates obtained by heating at C=40 g/L and C=70 g/L were first concentrated by ultrafiltration. Fig. 8a shows that in each case η_0 increased exponentially up to approximately 0.03 Pa.s: $\eta_0=\eta_s\exp(C/C_c)$, with η_s the solvent viscosity. The exponential increase obtained for the different aggregates superimposed when η_0 was plotted as a function of C/C_c, see fig. 8b. C_c decreased weakly with increasing aggregate size from C_c=35 g/L for $M_w=1.5\text{x}10^6$ g/mol to C_c=16.5 g/L for $M_w=1.1\text{x}10^8$ g/mol, see inset of fig. 8b.

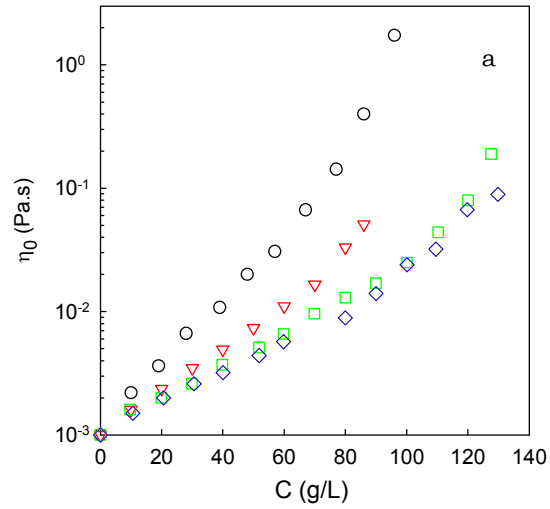

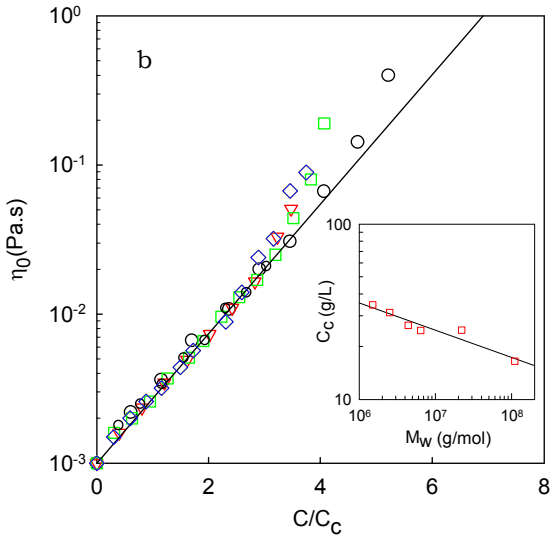

Fig. 8a Concentration dependence of η_0 for solutions of β-lg aggregates with different molar masses indicated in the figure.

Fig. 8b Master curve of the results shown in fig. 8a obtained by dividing C with C_c. The solid line represents $\eta_0=\eta_s.exp(C/C_c)$. The dependence of C_c on M_w is shown in the inset, which also includes results obtained for 2 other aggregate sizes for which the concentration dependence was not shown for clarity.

At higher protein concentrations, η_0 increased more steeply until it diverged and a gel was formed. We also observed that at these higher concentrations the viscosity increased slowly with time and in some cases weak gels were formed with time. It appears that bonds formed slowly between aggregates in these dense protein aggregate suspensions causing a rise

in the viscosity or gelation. This phenomenon of so-called cold gelation is well known to occur when electrostatic repulsion is reduced by adding salt or reducing the pH [1]. The rate of gelation increased with increasing aggregate concentration, but for all systems studied here the effects on the viscosity was negligible during the first two days. Notice, however, that the scattering intensity and ξ_d were stable even if gels were formed, implying that formation of the bonds occurred without a significant change in the structure of the solutions.

We have compared the behavior of large fractal aggregates with that of homogeneous microgels. As was discussed in ref.[29], microgels can be formed by heating β-lg solutions in the presence of a small amount of $CaCl_2$. For the present investigation the microgels were formed by heating a β-lg solution at C=40 g/L in the presence of 4.5mM $CaCl_2$. With light scattering techniques the following characteristics were obtained: M_w=1.1x10^9 g/mol, R_h=160 nm, R_g=200 nm. The structure of concentrated microgel suspensions could not be studied using light scattering, because they were highly turbid. In fig.9 the concentration dependence of η_0 of microgels is compared to that of the fractal aggregates. The viscosity of the fractal aggregate solutions increased more steeply with increasing protein concentration than for the microgel solutions, which was expected because the density of the latter is higher. However, the concentration dependence of the viscosity of the microgel solutions is still much larger than that of native proteins.

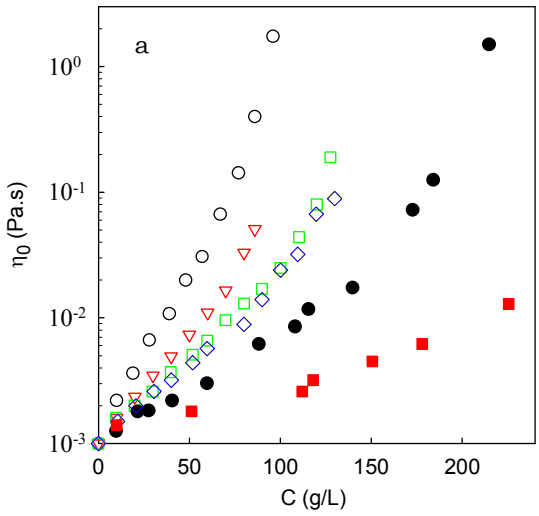

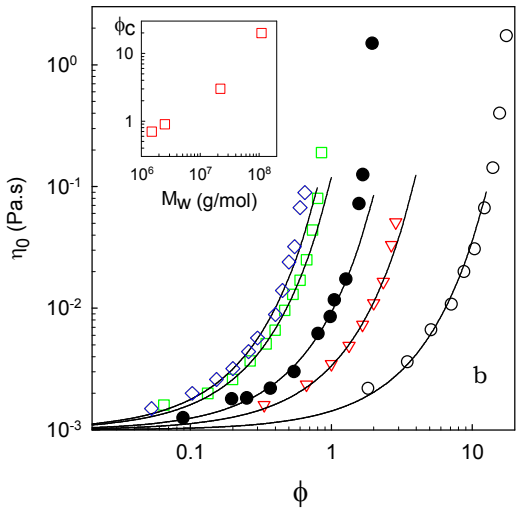

Fig. 9 Dependence of the zero shear viscosity on the concentration (a) or the volume fraction (b) of solutions of fractal aggregates (open symbols) and microgels (filled symbols). For comparison the concentration dependence of the viscosity of native β-lg is shown in fig. 9a (filled squares). Note that in fig. 9b the horizontal axis is logarithmic. The solid lines in fig. 9b represent exponential increases of η_0 with ϕ. Different open symbols represent different molar masses as indicated in fig 8.The inset of fig. 9b shows the molar mass dependence of ϕ_c.

Alternatively, we may compare the viscosity as a function of the effective volume fraction calculated as $\phi_e=C/C^*$. In fig. 9b, η_0 is plotted as a function of ϕ_e with C* calculated using in eq. 9 the hydrodynamic radius. The values of C* calculated in this way are shown in fig. 4 for the fractal aggregates and for the microgels C*=110 g/L. In this representation, the viscosity of the microgel suspensions increased more steeply than for fractal aggregates with $M_w=1.1x10^8$ g/mol and $M_w=2.2x10^7$ g/mol, but less steeply than for the smaller aggregates. η_0 diverged at $\phi_c=C_c/C^*\approx2$ for the microgels and $\phi_c\approx20$, 3, 0.9 and 0.7 for the fractal aggregates with $M_w= 1.1x10^8$, $2.2x10^7$, $2.5x\ 10^6$, and $1.5x10^6$ g/mol, respectively, see inset of fig. 9b. Except for the smallest aggregates, ϕ_c is larger than that of monodisperse hard spheres for which the viscosity diverges close to random close packing ($\phi_c=0.63$).

In part this can be explained by the polydispersity of the aggregates, which is large because they were formed by a random reaction limited aggregation process [3]. As was mentioned above, the values of R_g and R_h obtained from light scattering are strongly weighted by the largest aggregates so that the calculated value of C* is too small and therefore φ_e is too

large. The overestimation of ϕ_e would have been even worse if R_g or A_2 had been used to calculate C*. The polydispersity of the fractal aggregates increases with increasing average size, which means that ϕ_e is increasingly overestimated. In fact, as was mentioned in the introduction, the smallest aggregates are not fractal, but relatively monodisperse curved strands and are the building blocks of the larger fractal aggregates. The microgels are much less polydisperse than the larger fractal aggregates so that the overestimation ϕ_e is less important.

A second reason for the large values of φ_e is that the protein particles are soft so that they can be compressed to some extent. Much more importantly, polydisperse fractal aggregates interpenetrate in dense suspensions and the smaller aggregates are embedded within the larger ones. This effect is more important for larger fractal aggregates. As a consequence, the increase of the viscosity at a given concentration by using fractal aggregates instead of microgels or by using larger instead of smaller fractal aggregates is much less important than might have been anticipated from the difference in C* calculated from M_w and R_h or R_g.

Discussion

We have compared the behavior of dense suspensions of two types of protein aggregates. In pure water relatively monodisperse protein strands were formed for C<50g/L, which were the elementary units of the larger fractal aggregates formed at higher concentrations. Aggregation of the strands was reaction controlled and led to increasing polydispersity with increasing aggregate size. Solutions of the fractal aggregates were transparent, because smaller aggregates were embedded in the larger aggregates in a hierarchical manner. In addition, electrostatic repulsion between the proteins induced a weak local order. Interpenetration of the fractal aggregates explains why the structure of dense suspensions was independent of the aggregate size. The osmotic compressibility and the correlation length of dense suspensions were determined by the interactions between the elementary units of the fractal aggregates, i.e. small protein strands.

Spherical microgels of globular proteins were formed by addition of a small amount of $CaCl_2$ before heating. They probably consist of densely cross-linked network of small strands [20, 30]. The molar mass of microgels is much larger than that of fractal aggregates of the same size and therefore they scatter much more light. In addition, they are much less polydisperse

and smaller microgels cannot penetrate larger ones. As a consequence, microgel suspensions were turbid at higher concentrations and the structure of dense suspensions could not be evaluated by light scattering techniques.

The viscosity of colloidal particles as a function of their concentration has been extensively studied in the past and the effects of their architecture and the interaction between the particles have been reviewed [10-13, 31]. The viscosity diverges at a critical volume fraction and the dependence on ϕ has often been described by the Krieger-Dougherty equation [32] or the Quemada model [33]: $\eta_0=\eta_s.(1-\phi/\phi_c)^{-2}$. For monodisperse hard spheres ϕ_c is the concentration of close-packing, but in order to account for the effects of polydispersity, interaction or softness of the colloids ϕ_c has often been considered as an adjustable parameter. The same equation has been used to describe the concentration dependence for rigid clusters of randomly aggregated colloids [14-17]. The critical volume fraction of the colloids was found to decrease with increasing size of the fractal aggregates, because the density of the fractal aggregates decreased.

Here we find that the concentration dependence of the viscosity of the protein aggregates is much better described by an exponential increase except close to ϕ_c. An exponential increase of the viscosity was also reported for dendrimers [34], polymeric micelles [35] and randomly aggregated star polymers[19]. The latter study is particularly relevant here, because it is the only investigation of the viscosity of interpenetrated randomly aggregated particles with flexible bonds. Similarly to the fractal protein aggregates, the osmotic compressibility of fractal aggregates of star polymers could be described by eq.8 up to $\varphi\approx0.4$ and decreased more slowly at higher concentrations. Also for this system, the osmotic compressibility at high concentrations was found to be independent of the size of the aggregates and was determined by the interaction between the elementary units of the aggregates, i.e. the star polymers. The behavior of flexible fractal aggregates is very different from that of the rigid clusters, mainly because they can interpenetrate, but also because they are soft. This means that the viscosity of such systems cannot be interpreted in terms of the cumulated volume fraction of the aggregates.

If size of the aggregates is increased at a fixed concentration, the effect on the viscosity will be different for fractal aggregates and microgels. For fractal aggregates the viscosity will increase with increasing aggregate size, because the density of the aggregates decreases. However, if larger microgels are formed at a fixed concentration the viscosity

remains the same, assuming that the polydispersity and softness of the microgels does not depend on their size, because the volume fraction remains the same. If the size of the aggregates increases with increasing concentration as was the case for the fractal aggregates formed at different concentrations, the viscosity increases very steeply due to the combined effects of increasing size and increasing concentration. Comparison of the two situations for globular protein aggregates showed that former effect was most important.

Conclusion

Fractal aggregates are formed by heating globular proteins in aqueous solutions at pH 7. The average aggregate size increases if the concentration at which the proteins are heated is increased and diverges at the critical gel concentration. For a given aggregate size the viscosity increases exponentially with the protein concentration. The increase is steeper if the aggregates are larger, because the density of the aggregates decreases with increasing size. However, the effect of the aggregate size is smaller than expected from the decrease of the density, because the aggregates are very polydisperse and smaller aggregates are embedded within the larger ones. The viscosity of protein solutions after heating at different concentrations rises very sharply over a small concentration range close to the critical gel concentration, because the average size of the aggregates rises sharply. The osmotic compressibility and the correlation length of the concentration fluctuations decrease with increasing concentration and are independent of the aggregate size at high concentrations, where they are determined by the interaction between the elementary units of the aggregates. The behaviour of aggregates formed by WPI is close to that for β-lg aggregates.

The behavior of microgels formed by heating globular proteins in the presence of a small amount of $CaCl_2$ is different from that of fractal aggregates, because they are denser and cannot interpenetrate. Therefore the increase of the viscosity of microgel solutions with increasing protein concentration is weaker and does not depend on the size of the microgels.

Acknowledgement W.I. acknowledges financial support from the office of eduction affairs, the ministry of science and technology and the national institute of metrology of Thailand.

References

1. T. Nicolai, M. Britten and C. Schmitt, *Food Hydrocolloids*, 2011, **25**, 1945-1962.

2. R. Mezzenga and P. Fischer, *Reports on Progress in Physics*, 2013, **76**, 046601.
3. J. C. Gimel, D. Durand and T. Nicolai, *Macromolecules*, 1994, **27**, 583-589.
4. N. Mahmoudi, S. Mehalebi, T. Nicolai, D. Durand and A. Riaublanc, *J. Agric. Food Chem.*, 2007, **55**, 3104-3111.
5. T. Hagiwara, H. Kumagai and K. Nakamura, *Bioscience, biotechnology, and biochemistry*, 1996, **60**, 1757-1763.
6. N. Micali, V. Villari, M. A. Castriciano, A. Romeo and L. Monsù Scolaro, *The Journal of Physical Chemistry B*, 2006, **110**, 8289-8295.
7. R. Vreeker, L. Hoekstra, D. Den Boer and W. Agterof, *Food Hydrocolloids*, 1992, **6**, 423-435.
8. M. Weijers, R. W. Visschers and T. Nicolai, *Macromolecules*, 2002, **35**, 4753-4762.
9. L. Donato, C. Garnier, J. L. Doublier and T. Nicolai, *Biomacromolecules*, 2005, **6**, 2157-2163.
10. D. B. Genovese, *Advances in Colloid and Interface Science*, 2012, **171-172**, 1-16.
11. D. Quemada and C. Berli, *Advances in Colloid and Interface Science*, 2002, **98**, 51-85.
12. F. Sciortino and P. Tartaglia, *Advances in Physics*, 2005, **54**, 471-524.
13. D. Vlassopoulos and M. Cloitre, *Current Opinion in Colloid & Interface Science*, 2014, **19**, 561-574.
14. T. Aubry, B. Largenton and M. Moan, *Journal of colloid and interface science*, 1998, **202**, 551-553.
15. I. R. Collins, *Journal of Colloid and Interface Science*, 1996, **178**, 361-363.
16. C. Tsenoglou, *J. Rheol.*, 1990, **34**, 15-24.
17. N. Kovalchuk, I. Kuchin, V. Starov and N. Uriev, *Colloid Journal*, 2010, **72**, 379-388.
18. K. Baussay, C. Le Bon, T. Nicolai, D. Durand and J. Busnel, *International Journal of biological Macromolecules*, 2004, **34**, 21-28.
19. R.-P. Nzé, T. Nicolai, C. Chassenieux, E. Nicol, S. Boye and A. Lederer, *Macromolecules*, 2015, **48**, 7995-8002.
20. T. Nicolai, *Colloids and Surfaces B: Biointerfaces*, 2015, **137**, 32-38.
21. M. Boland, H. Singh and A. Thompson, *Milk proteins: from expression to food*, Academic Press, 2014.
22. W. Brown, *Light Scattering. Principles and Developments*, Clarendon Press, Oxford, 1996.
23. J. S. Higgins and K. C. Benoit, *Polymer and Neutron Scattering*, Clarendon Press, Oxford, 1994.
24. B. Berne and R. Pecora, *Dynamic light scattering With Applications to Chemistry, Biology, and physics*, Dover Publications, New York, 2000.
25. W. Brown, *Dynamic Light Scattering: The method and some applications*, Clarendon Press Oxford, 1993.
26. V. Sharma, A. Jaishankar, Y.-C. Wang and G. H. McKinley, *Soft Matter*, 2011, **7**, 5150-5160.
27. M. Pouzot, T. Nicolai, R. W. Visschers and M. Weijers, *Food Hydrocolloids*, 2005, **19**, 231-238.
28. N. F. Carnahan and K. E. Starling, *Journal of Chemical Physics*, 1969, **51**, 635-636.
29. T. Phan-Xuan, D. Durand, T. Nicolai, L. Donato, C. Schmitt and L. Bovetto, *Food Hydrocolloids*, 2014, **34**, 227-235.
30. C. Schmitt, C. Moitzi, C. Bovay, M. Rouvet, L. Bovetto, L. Donato, M. E. Leser, P. Schurtenberger and A. Stradner, *Soft Matter*, 2010, **6**, 4876-4876.
31. D. Vlassopoulos and G. Fytas, in *High Solid Dispersions*, Springer Berlin Heidelberg, 2010, vol. 236, pp. 1-54.
32. I. M. Krieger, *Adv. Coll. Int. Sci.*, 1972, **3**, 111-136.
33. D. Quemada, *Rheologica Acta*, 1977, **16**, 82-94.
34. I. B. Rietveld and D. Bedeaux, *Journal of colloid and interface science*, 2001, **235**, 89-92.
35. N. Merlet-Lacroix, E. Di Cola and M. Cloitre, *Soft Matter*, 2010, **6**, 984-993.

For TOC only

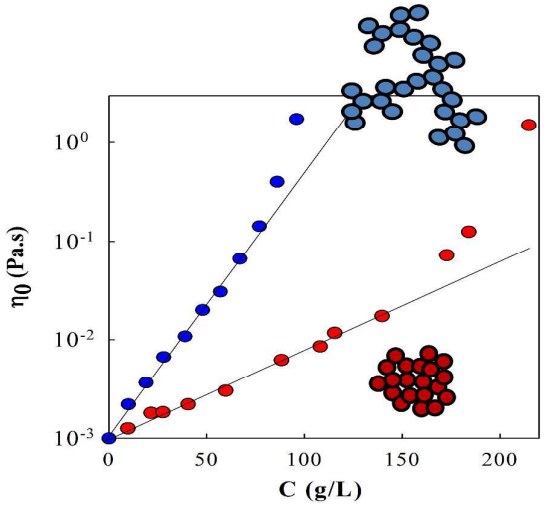

Zero-shear viscosity as a function of the protein concentration for fractal aggregates and microgels.